Molecular Cancer Therapeutics

Acquired Resistance to the Hsp90 Inhibitor, Ganetespib, in *KRAS*-Mutant NSCLC Is Mediated via Reactivation of the ERK–p90RSK–mTOR Signaling Network

Suman Chatterjee[1], Eric H.-B. Huang[1], Ian Christie[1], Brenda F. Kurland[2], and Timothy F. Burns[1]

Abstract

Approximately 25% of non–small cell lung cancer (NSCLC) patients have *KRAS* mutations, and no effective therapeutic strategy exists for these patients. The use of Hsp90 inhibitors in *KRAS*-mutant NSCLC appeared to be a promising approach, as these inhibitors target many KRAS downstream effectors; however, limited clinical efficacy has been observed due to resistance. Here, we examined the mechanism(s) of acquired resistance to the Hsp90 inhibitor, ganetespib, and identified novel and rationally devised Hsp90 inhibitor combinations, which may prevent and overcome resistance to Hsp90 inhibitors. We derived *KRAS*-mutant NSCLC ganetespib-resistant cell lines to identify the resistance mechanism(s) and identified hyperactivation of RAF/MEK/ERK/RSK and PI3K/AKT/mTOR pathways as key resistance mechanisms. Furthermore, we found that ganetespib-resistant cells are "addicted" to these pathways, as ganetespib resistance leads to synthetic lethality to a dual PI3K/mTOR, a PI3K, or an ERK inhibitor. Interestingly, the levels and activity of a key activator of the mTOR pathway and an ERK downstream target, p90 ribosomal S6 kinase (RSK), were also increased in the ganetespib-resistant cells. Genetic or pharmacologic inhibition of p90RSK in ganetespib-resistant cells restored sensitivity to ganetespib, whereas p90RSK overexpression induced ganetespib resistance in naïve cells, validating p90RSK as a mediator of resistance and a novel therapeutic target. Our studies offer a way forward for Hsp90 inhibitors through the rational design of Hsp90 inhibitor combinations that may prevent and/or overcome resistance to Hsp90 inhibitors, providing an effective therapeutic strategy for *KRAS*-mutant NSCLC. *Mol Cancer Ther; 16(5); 793–804. ©2017 AACR.*

Introduction

In 2015, approximately 160,340 lung cancer–related deaths occurred in the United States alone (1). Despite recent advances in lung cancer treatment, it remains the leading cause of cancer-related deaths in the United States and worldwide, and the 5-year survival rate is still below 20%. Although the discovery of driver oncogenes has revolutionized lung cancer therapeutics, no effective therapies exist for the oncogenic driver *KRAS* mutation (2–4), which is present in approximately 25% of non–small cell lung cancer (NSCLC) patients' tumors. Patients with *KRAS*-mutant lung cancer have worst outcomes in early-stage disease and a poor prognosis in the metastatic setting (3). There is a critical need for novel agents targeting *KRAS*-mutant NSCLC.

Hsp90 is an ATP-dependent molecular chaperone required for the stability of its "client" oncoproteins, many of which are effectors of KRAS, such as members of RAF/ERK and PI3K/AKT/mTOR pathways (5). The critical role of Hsp90 in tumorigenesis led to the development of several first- and second-generation Hsp90 inhibitors (Hsp90i), which demonstrated promising responses in oncogene-driven cancers, such as *HER2*$^+$ breast cancer (6). Ganetespib, a second-generation small-molecule Hsp90i, has shown significant single-agent activity in ALK-driven disease, but only transient, unconfirmed responses were observed in patients with *KRAS*-mutant tumors (7, 8). Therefore, identifying acquired resistance mechanism(s) to ganetespib in *KRAS*-mutant NSCLC may allow for the development of an effective therapeutic strategy for *KRAS*-mutant NSCLC.

Here, we have characterized the mechanism(s) of acquired resistance to ganetespib by generating and analyzing multiple ganetespib-resistant *KRAS*-mutant NSCLC cell lines. We found that hyperactivation of RAF/MEK/ERK and PI3K/AKT/mTOR signaling is a key component of acquired ganetespib resistance. Moreover, our results strongly implicate the ERK pathway and the ERK target, p90RSK, an important serine/threonine kinase, as central mediators of this resistance. We have also examined potential combinatorial activity of ganetespib with inhibitors targeting critical signaling molecules of these pathways. Overall, our preclinical data provide the justification for future clinical trials involving rationally designed Hsp90i combinations that may be effective against *KRAS*-mutant NSCLC.

[1]Department of Medicine, Division of Hematology Oncology, University of Pittsburgh Cancer Institute, Pittsburgh, Pennsylvania. [2]Department of Biostatistics, University of Pittsburgh, Pittsburgh, Pennsylvania.

Note: Supplementary data for this article are available at Molecular Cancer Therapeutics Online (http://mct.aacrjournals.org/).

Corresponding Author: Timothy F. Burns, Department of Medicine, Division of Hematology-Oncology, University of Pittsburgh, 5117 Centre Avenue, HCCRP, Suite 2.18e, Pittsburgh, PA 15213. Phone: 412-864-7859; Fax: 412-623-7798; E-mail: burnstf@upmc.edu

doi: 10.1158/1535-7163.MCT-16-0677

Materials and Methods

Cell lines and reagents

Seven human *KRAS*-mutant NSCLC cell lines (A549, H460, H358, H727, H23, Calu-6, and SW1573) and embryonic kidney cell line HEK 293T were acquired in 2013 from the ATCC and maintained in ATCC-specified growth medium. All cell lines were authenticated by autosomal STR (short tandem repeat) profiling done at University of Arizona Genetics Core. Z-VAD-FMK was purchased from R&D Systems. Ganetespib and PX-866 were generously gifted by Synta Pharmaceutical Corp. and Dr. Peter Wipf's laboratory (University of Pittsburgh, Pittsburgh, PA), respectively. 17-AAG and NVP-BEZ235 were purchased from LC Laboratories, onalespib (AT13387), gedatolisib (PF-05212384, PKI-587), SCH772984, and BI-D1870 from Selleck Chemicals, SL0101 from Calbiochem, and docetaxel from Sigma-Aldrich.

Generation of ganetespib-resistant *KRAS*-mutant NSCLC cell lines

To derive our ganetespib-resistant cell lines, we used low-dose (IC_{25} and below) continuous treatments with gradually increasing doses, which allowed the development of ganetespib-resistant cell lines in approximately 3 months. The maximum dose of ganetespib at which A549-GR100 cells survive with negligible cell death was 100 nmol/L. H460-GR10 and H358-GR10 could not survive beyond 10 nmol/L ganetespib dose and are hence named GR10s. Ganetespib resistance of these ganetespib-resistant cells was tested in comparison with their parental stocks every second week. Once resistance was confirmed, these cells were always maintained in their respective ganetespib doses.

Cell proliferation assays

Cell viability after treatment was determined using the CellTiter96 Aqueous One Solution Cell Proliferation Assay Kit (Promega) according to the manufacturer's protocol. Quadruplets were used for each treatment group, and data were normalized to percentage of controls. IC_{50} values were calculated using Prism V5.0 (GraphPad software). Colony formation assays were performed as described previously (9). For cell proliferation studies, at least three independent experiments were performed.

Western blot analysis and antibodies

After being treated with specific drugs for defined periods of times, cell collection, protein preparation, concentration measurements, and Western blotting were performed as described previously (9). Information on all antibodies used in this report is provided in Supplementary Table S1.

Lentiviral shRNA and cDNA overexpression

293T cells (4×10^6) were seeded in 25-cm^2 flasks and were transfected to generate lentiviral particles using a four-plasmid system as per the TRC Library Production and Performance protocols, RNAi Consortium, Broad Institute (10), and as described previously (9). p90RSK shRNA constructs were purchased from Johns Hopkins University HiT Center (Baltimore, MD), and their respective sequences are listed in Supplementary Table S2. pLKO.1-shRNA scramble vector was obtained from Dr. David M. Sabatini (Whitehead Institute for Biomedical Research, Cambridge, MA) through Addgene (Addgene plasmid 1864) as described previously (11). The pLenti CMV Puro DEST (w118-1) vector was obtained from Eric Campeau (University of Massachusetts Medical School, Worchester, MA) through Addgene (Addgene plasmid 17452). The Ultimate ORFs (Invitrogen) for RSK1-4 were obtained from the Johns Hopkins University HiT Center, and an LR reaction (Invitrogen) was performed to construct pLenti Puro DEST (w118-1)-RSK 1-4. All constructs were sequence verified. The ORF clone IDs of the constructs are IOH46696 (RSK1.a, variant 1), IOH12130 (RSK1.b, variant 2), IOH63248 (RSK2), IOH3648 (RSK3), and IOH36120 (RSK4).

In vivo experiments

For A549 xenografts, a total of 5×10^6 viable cells were suspended in equal volumes of PBS and Matrigel and subcutaneously injected in adult 6- to 8-week-old athymic nude mice [Crl:NU (NCr)-F; Charles River Laboratories). Once the tumors reached an average size of $\geq$150 mm^3 (range, 100–250 mm^3), mice were distributed among control and treatment arms and were intravenously dosed with either vehicle control or ganetespib 100 mg/kg once a week. Tumor sizes [$1/2(\text{length} \times \text{width}^2)$] were measured by digital caliper twice a week. In addition, we used a *KRAS*-mutant human patient-derived xenograft (PDX) model established from a specimen of brain metastasis (BM012-15) from a patient with *KRAS* G12C mutation. Tumor tissues (2 mm^2) cut with sterile blade were implanted subcutaneously. Once reaching $\geq$150 mm^3, animals were randomized to 2 arms and intravenously dosed with vehicle control or ganetespib (50 mg/kg). Animals were sacrificed once tumors reached approximately 2,000 mm^3.

Statistical analyses

Group comparisons in cell line studies were conducted using Student *t* test. Growth patterns in animal studies were summarized graphically by plotting the mean and SE for each treatment group at each tumor assessment time. Random intercept linear mixed models were used to predict log (base 2) of tumor volume. Residual plots and influence statistics were examined to ensure that model assumptions, such as log-linear growth, were not violated. Statistical analyses were conducted using SAS/STAT software, version 9.4 (SAS Institute, Inc.), and reported *P* values were two-sided.

Results

Ganetespib inhibits growth of *KRAS*-mutant NSCLC cells and reduces the expression and activity of RAF/MEK/ERK and PI3K/AKT/mTOR signaling pathways

We first established the relative efficacy of the drug *in vitro* in a panel of *KRAS*-mutant NSCLC cell lines. Representative viability curves after ganetespib treatment are shown for all 7 lines at 72 hours in Fig. 1A (left). In accordance with previous studies (12), ganetespib exhibited potent cytotoxicity with low nanomolar range of IC_{50} values (31–67 nmol/L) tabulated in Fig. 1A (right). Ganetespib was also efficacious in two distinct *in vivo* models harboring *KRAS* mutation. Ganetespib induced notable tumor growth inhibition both in the *KRAS*-mutant (G12S) A549 xenograft model (Fig. 1B, left), as well as in our *KRAS*-mutant (G12C) PDX model (Fig. 1B, right). Using a random intercept linear mixed model predicting log (base 2) of tumor volume, the predicted average doubling time for the A549 model was 24 days [95% confidence interval (CI), 17–44] for ganetespib and 9 days (95% CI, 8–11) for the vector (Wald test; ***, $P < 0.001$). For the PDX, the fitted doubling times were 6 days (95% CI, 5–6) for ganetespib and 4 days (95% CI, 4–5) for the vector (Wald test; ***, $P < 0.001$).

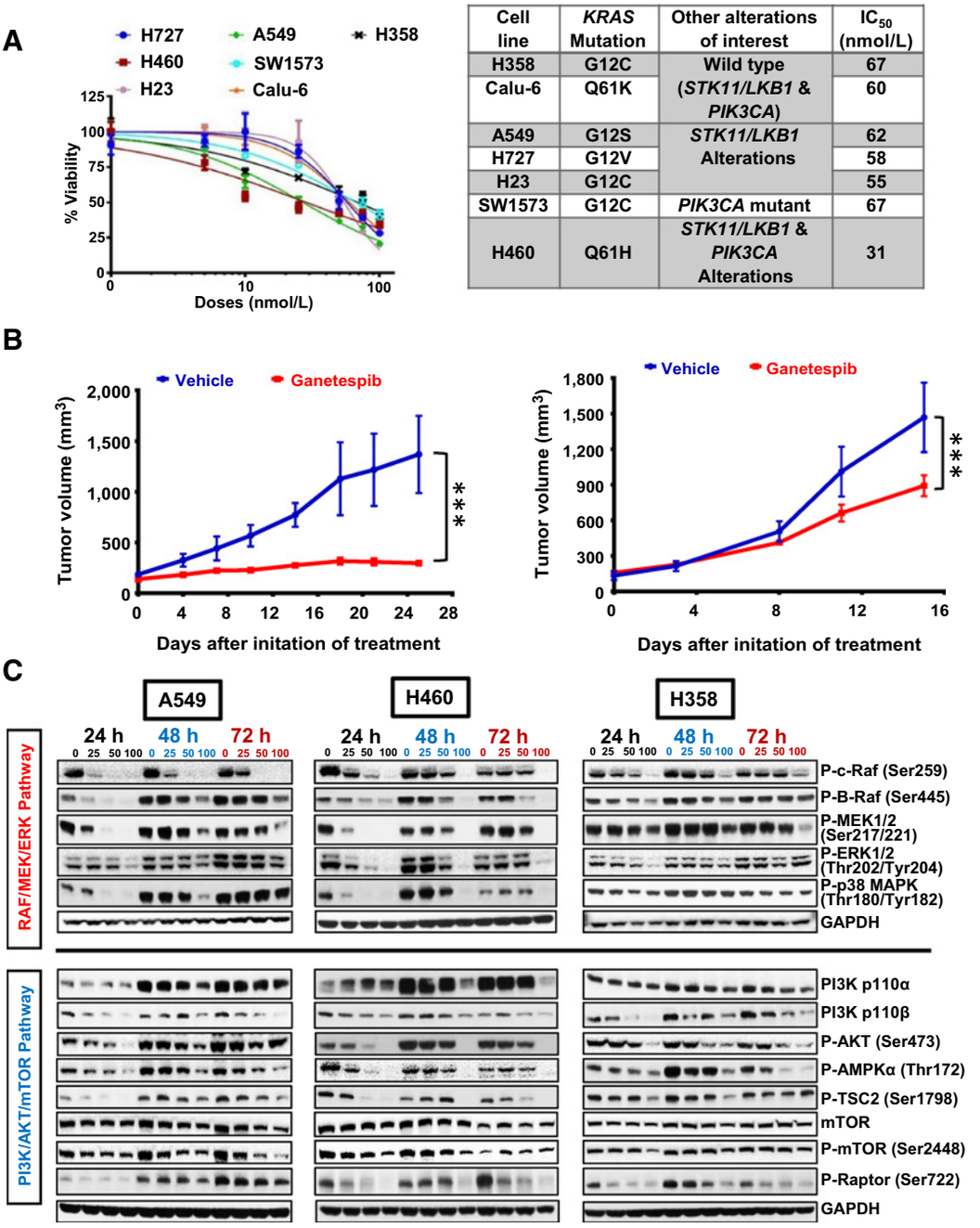

Cell line	*KRAS* Mutation	Other alterations of interest	IC_{50} (nmol/L)
H358	G12C	Wild type	67
Calu-6	Q61K	(*STK11/LKB1* & *PIK3CA*)	60
A549	G12S	*STK11/LKB1* Alterations	62
H727	G12V		58
H23	G12C		55
SW1573	G12C	*PIK3CA* mutant	67
H460	Q61H	*STK11/LKB1* & *PIK3CA* Alterations	31

Figure 1.

Ganetespib inhibits cell growth and decreases the protein expression levels of RAF/MEK/ERK and PI3K/AKT/mTOR pathway members in *KRAS*-mutant NSCLC cell lines. **A,** Cells were treated with ganetespib (0–500 nmol/L), and viability was measured after 72 hours by MTS assay (top left). The IC_{50} values of the seven *KRAS*-mutant NSCLC cell lines grouped according to their *STK11/LKB1* and *PIK3CA* mutational status are tabulated (top right). **B,** *In vivo* efficacy of ganetespib was assessed in a *KRAS*-mutant NSCLC (A549; *KRAS* mutation: G12S) xenograft model (left), as well as in the *KRAS*-mutant (G12C) PDX model (BM012-15) (right). Tumor growth curves represent mean tumor volume (±SEM). $n = 5$ mice in vehicle, and 4 in ganetespib arms in xenograft model. Four mice in vehicle, and 5 in ganetespib arms in PDX model. Ganetespib displayed significant efficacy (***, $P < 0.001$). **C,** A549, H460 and H358 cells were treated with increasing doses of ganetespib for 24, 48, and 72 hours, and expression of RAF/MEK/ERK and PI3K/AKT/mTOR family member proteins were assessed by immunoblotting. GAPDH was included as loading control.

Next, we examined the effect of ganetespib on the expression of several Hsp90 clients in the RAF/MEK/ERK and PI3K/AKT/mTOR pathways. Three representative *KRAS*-mutant cell lines A549, H460, and H358 were treated with increasing doses of ganetespib and expression of Hsp90 clients, and other related proteins were profiled by immunoblotting. Our results suggest that the

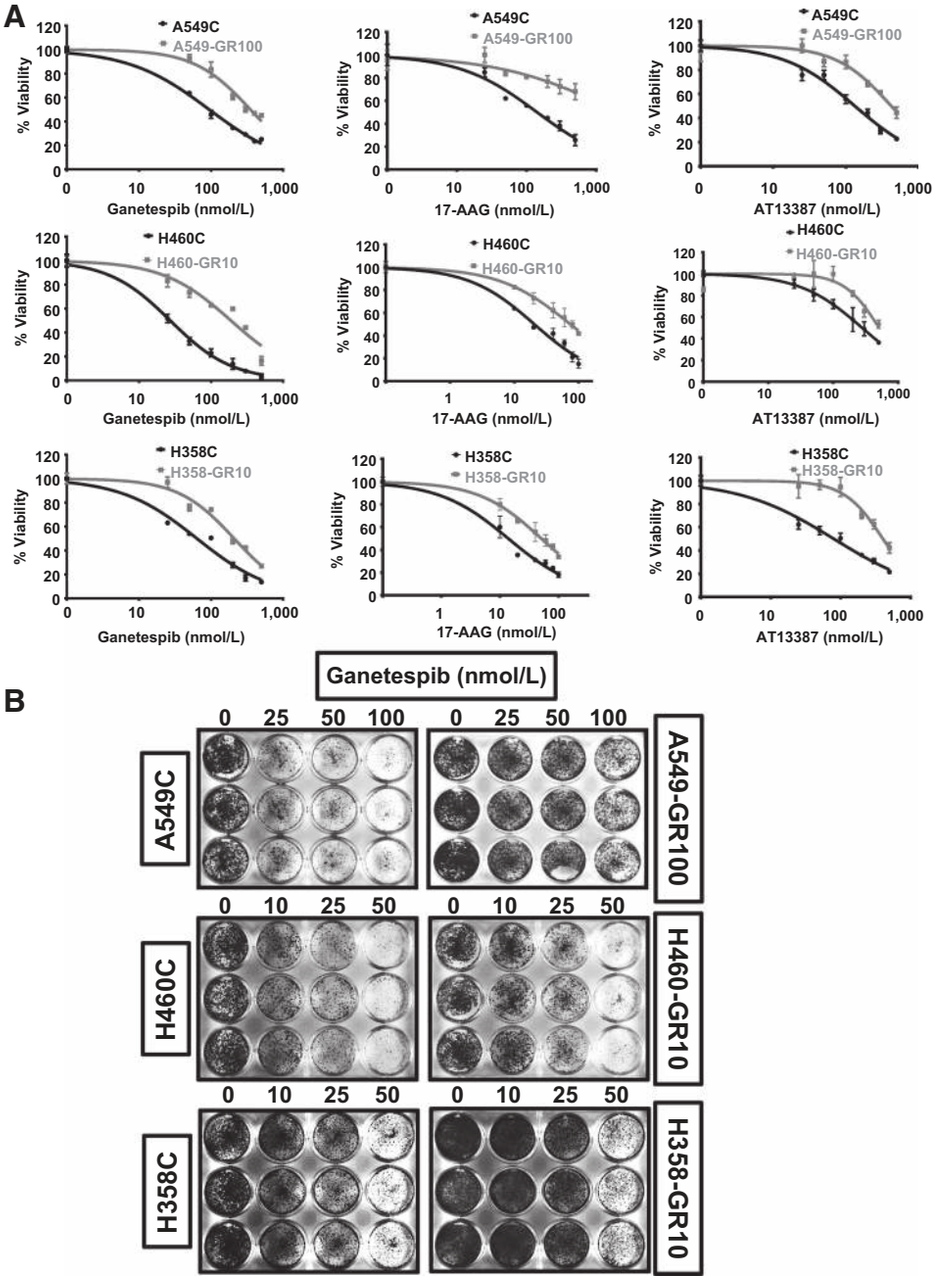

Figure 2.
Derivation and analysis of acquired ganetespib-resistant cells from parental A549, H460, and H358 cell lines. **A,** A549-GR100, H460-GR10, and H358-GR10 cells were exposed to ganetespib, and cell viability was assessed by MTS assay after 72 hours in comparison with their respective parental control cells (denoted by C; left). Cell viability was also assessed 48 hours after treating the same three pairs of cells with 17-AAG (middle) and AT13387 (right). **B,** Durability of ganetespib resistance was confirmed by long-term colony formation assay in A549-GR100, H460-GR10, and H358-GR10 cells growing the cell lines in ganetespib at the indicated doses for 3 days and staining on day 10.

expression and activity of RAF/ERK and PI3K/AKT/mTOR family members are notably diminished after ganetespib treatment (Fig. 1C; Supplementary Fig. S1). In addition, crucial upstream mTOR regulators, such as PI3K p110 subunits α and β, P-AKT, P-TSC2, and P-AMPKα, were also markedly inhibited by ganetespib.

Derivation and characterization of ganetespib-resistant *KRAS*-mutant NSCLC cells

To derive ganetespib-resistant cell lines, we initiated low-dose (IC_{25} and below) continuous treatment with gradually increasing doses of ganetespib treatment. As shown in Fig. 2, we have successfully developed A549-GR100 (resistant up to 100 nmol/L ganetespib), H460-GR10, and H358-GR10 (resistant up to 10 nmol/L ganetespib) cell lines. Our Hill slope curve analysis indicated IC_{50} values of 61.7 nmol/L for the parental A549 and 337.1 nmol/L for the A549-GR100 cells, 31 nmol/L for the parental H460 and 178.8 nmol/L for the H460-GR10 cells, 67.1 nmol/L for the parental H358 and 193.7 nmol/L for the H358-GR10 cell lines, respectively (Fig. 2A; Supplementary Table S3). To examine the durability of our ganetespib-resistant cells, we performed long-term colony formation assay and observed increased viability of ganetespib-resistant cells compared with parental cells with increasing doses of ganetespib (Fig. 2B). Differential sensitivity of specific cancer types to Hsp90is owing to their differential drug

metabolism properties has been reported (13). Therefore, to rule out that the observed resistance was not simply due to altered ganetespib metabolism, we examined the responses of our ganetespib-resistant cell lines to Hsp90is with different metabolic pathways. We found that in addition to being resistant to ganetespib (Fig. 2A, left), ganetespib-resistant cell lines showed cross-resistance to the first-generation ansamycin compound, 17-AAG (Fig. 2A, middle) as well as to another second-generation Hsp90i, AT13387 (Fig. 2A, right). These results suggest that resistance is not just due to differential drug metabolism in our resistance cells. We next asked whether the Hsp90 chaperone machinery was still functional in our ganetespib-resistant cells and whether ganetespib was still able to engage the Hsp90 machinery. As the induction of Hsp90 and Hsp70 expression in response to Hsp90 inhibition is a well-established compensatory mechanism within the cell (6), we examined whether this response was intact in our ganetespib-resistant cells. After ganetespib treatment, we observed increased expression of both Hsp90 and Hsp70 in the parental and ganetespib-resistant cells (Supplementary Fig.S2). Often times, this is accompanied by an increase in the heat shock factor 1 (HSF1) transcription factor (6). In our cells, we observed a modest increase in both the parental and ganetespib-resistant A549 cells but failed to see an increase in our H460 ganetespib-resistant cells after ganetespib likely secondary to marked increased baseline levels that were present. We also examined whether selected Hsp90 client proteins were still degraded in the presence of ganetespib in our resistant cells. Although the baseline expression of active GSK-3-β, a well-known Hsp90 client protein (14, 15), was significantly higher in ganetespib-resistant cells, in both control and ganetespib-resistant cells, the GSK-3-β activity reduced in a dose-dependent manner, further corroborating the fact that the Hsp90 chaperonage is active in our ganetespib-resistant system.

Ganetespib resistance leads to hyperactivation of the RAF/MEK/ERK and AKT/mTOR signaling in *KRAS*-mutant NSCLC and dependence on the ERK and PI3K/mTOR pathways

As we observed marked reduction in expression of the ERK and mTOR pathway members in our parental *KRAS*-mutant cells in response to ganetespib (Fig. 1C), we analyzed the expression and activity of the members of these pathways in our control and ganetespib-resistant *KRAS*-mutant cells. Surprisingly, we observed notable reactivation/stabilization of RAF/MEK/ERK (Fig. 3) and PI3K/AKT/mTOR (Fig. 4; Supplementary Fig. S3) pathway members in our ganetespib-resistant lines. Although KRAS is not a known Hsp90 client and has been previously reported to be unaffected by ganetespib treatment (12), for the first time, here we report that mutant KRAS expression is also altered by ganetespib treatment. Utilizing KRAS-mutant–specific antibodies, we observed elevated expressions of mutant KRAS (G12S in A549 and Q61H in H460) compared with controls (Fig. 3A). Our results suggest that upregulation of the RAF/MEK/ERK as well as the PI3K/AKT/mTOR pathways may mediate resistance to ganetespib.

We next examined the requirement for RAF/MEK/ERK activity in ganetespib resistance using the potent, ATP-competitive and noncompetitive inhibitor of ERK1/2, SCH772984 (16, 17). Both A549 and H460 ganetespib-resistant cells, when treated with increasing concentration of the drug, compared with parental cells, showed greater sensitivity to SCH772984 (Fig. 3B). SCH772984 IC_{50} was determined to be 5.7 μmol/L in A549C cells compared with 1.7 μmol/L in A549-GR100 cells and 6.1 μmol/L in H460C cells compared with 2.0 μmol/L in H460-GR10 cells (Supplementary Table S3). These results suggest that ganetespib resistance leads to increased dependence on the ERK signaling pathway. We next investigated whether the combination of Hsp90 and ERK inhibition in parental cells would lead to synergistic growth inhibition. We failed to detect a synergistic interaction, but rather, a strong additive combinatorial activity was observed in Loewe excess matrices for ganetespib with SCH772984 (data not shown). To validate the combinatorial activity of ganetespib and SCH772984, we selected specific dose combinations on the basis of the Loewe excess matrices results. We observed a strong additive effect in A549 parental cells for the combination of 500 nmol/L SCH772984 and 50 to 75 nmol/L ganetespib as compared with control ($P < 0.05$; Fig. 3C). In addition to other important kinases like AKT (18, 19), ERK1/2 is also known to lead to activation of the mTOR pathway (Supplementary Fig. S4A; ref. 20). Therefore, we assessed the ability of SCH772984 to inhibit mTOR signaling in control versus ganetespib-resistant cells. Surprisingly, even in the presence of uninhibited AKT signaling, SCH772984 was able to affect the expression of several mTOR pathway proteins (Supplementary Fig. S4B), supporting the potential efficacy of the combination of SCH772984 and ganetespib.

We next examined the dependence of ganetespib-resistant cells on PI3K/AKT/mTOR pathway by treating the parental and ganetespib-resistant cells with the dual PI3K/mTOR inhibitors BEZ235 (Fig. 4B) and PF-05212384 (Supplementary Fig. S3B), or the PI3K inhibitor, PX-866 (Fig. 4C). Remarkably, we observed increased dependence on this pathway as well as synthetic lethality to these drugs in the ganetespib-resistant cells (respective IC_{50} values are tabulated in Supplementary Table S3). As our panel of ganetespib-resistant cells showed synthetic lethality to these drugs, we decided to further analyze the efficacy of PF-05212384, which is currently in clinical development, in combination with ganetespib in our control parental cells. On the basis of our preliminary results of Loewe excess matrices (data not shown) for ganetespib with PF-05212384, we tested the efficacy of the combination in A549-naïve cells. We selected specific dose combinations on the basis of the Loewe excess matrices. Our results indicated a strong additive effect of the 10 nmol/L PF-05212384 in combination with either 50 or 75 nmol/L ganetespib, compared with ganetespib treatment alone (Supplementary Fig. S3C).

p90RSK, the key ERK substrate and an activator of the mTOR signaling pathway, plays an essential key role in mediating the acquired resistance to ganetespib

Simultaneous increased activity of the RAF/MEK/ERK pathway as well as mTOR pathway members in ganetespib-resistant *KRAS*-mutant cells in the presence of ganetespib led to the question of what signaling molecule mediates the cross-talk between the two pathways. Upon activation, ERK1/2 targets multiple downstream mediators, including the p90RSK (90 kDa ribosomal S6 kinase) family proteins (21, 22). This protein has four human isoforms (p90RSK1–4), among which both RSK1 and RSK2 have been reported to activate/phosphorylate the regulatory associated protein of mTOR (RAPTOR), which is required for the mTORC1 complex activity (22, 23). Hence, we investigated the involvement, if any, of this protein in ganetespib resistance. Remarkably, we observed significantly higher p90RSK activity as indicated by

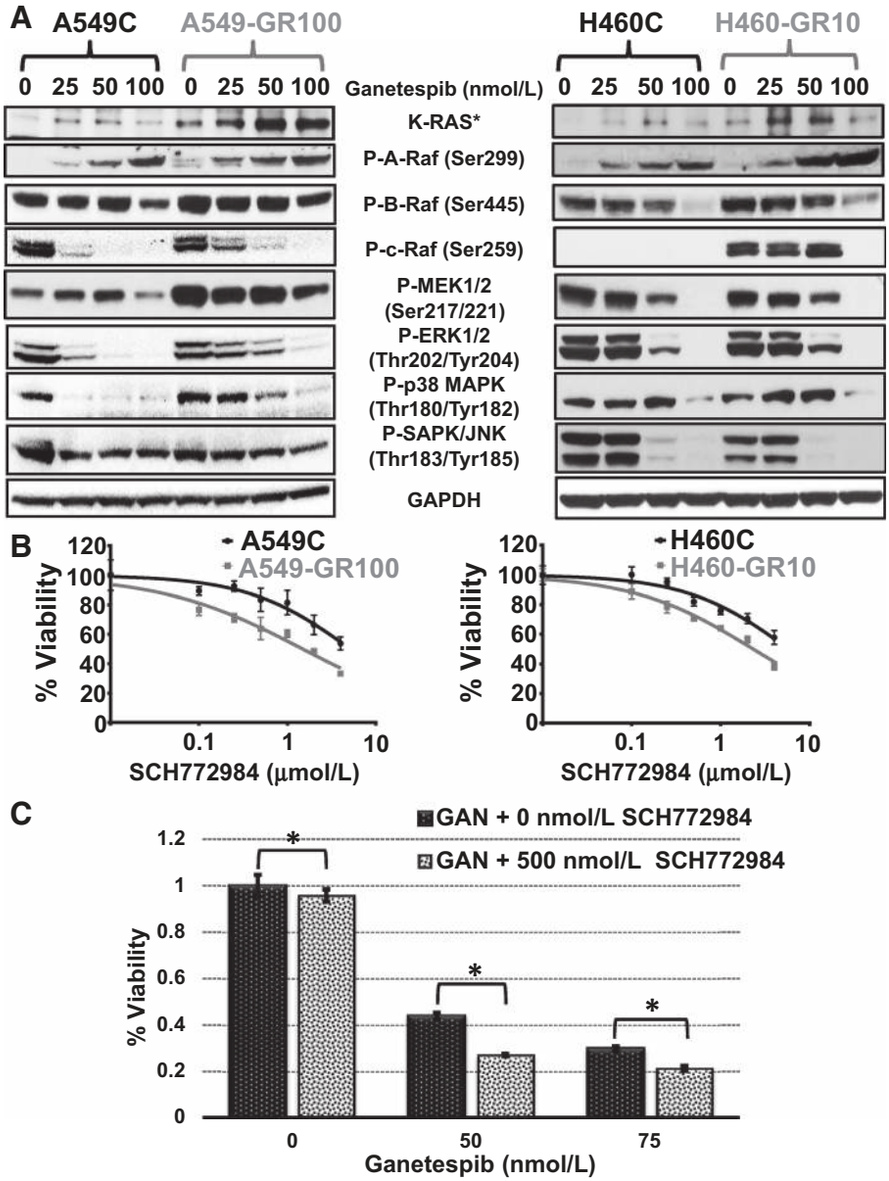

Figure 3.
Acquired resistance to ganetespib induces hyperactivation of the RAF/MEK/ERK pathway leading to ERK dependence. **A,** Expression of mutant KRAS and members of RAF/MEK/ERK pathway was compared by immunoblotting in control (C) versus ganetespib-resistant cells, after treatment with ganetespib for 48 hours (*antibodies against A549-specific G12S and H460-specific Q61H were used for respective comparisons). GAPDH was included as loading control. **B,** Percent viability of ganetespib-resistant and control cells in response to 72 hours treatment with SCH772984 (0–4 μmol/L) were analyzed by MTS assay. **C,** A549 cells were treated with increasing concentrations of ganetespib (0–100 nmol/L) in the absence or presence of 500 nmol/L SCH772984 for 48 hours, followed by MTS assay to determine the percent viability of the cells. Bars represent the mean percent cell viability (±SD) relative to the mean of control cells (DMSO). Each cell type in each experiment included at least four replicates. Statistical significance by unpaired Student *t* test is denoted as *, $P < 0.05$.

the levels of S380 phosphorylation in ganetespib-resistant cells compared with controls (Fig. 5A). This evolutionary conserved protein is not only activated by sequential phosphorylation by ERK1/2, but also requires PDK1 phosphorylation, which is essential for its activation (Fig. 5B; ref. 24). We observed increased levels of total and P-PDK in the ganetespib-resistant cells as well (Supplementary Fig. S3A). Next, we investigated whether the expression and activity of individual isoforms differed in our control versus ganetespib-resistant cell lines (Fig. 5C). Although, the basal expression levels of the p90RSK isoforms in ganetespib-resistant cells were not markedly higher than that in their respective control cells, the levels of expression for both total and phosphorylated forms were increased for a subset of p90RSK isoforms in ganetespib-resistant cells compared with their respective controls. In addition, a subset of p90RSK isoforms is induced in a ganetespib dose–dependent manner, suggesting that the p90RSK isoforms are primed to be induced in response to increasing Hsp90 inhibition. These findings are concordant with the observed increased activity of P-ERK1/2 (Fig. 3) and P-PDK1 (Supplementary Fig. S3A) in ganetespib-resistant cells in the presence of ganetespib and place p90RSK as the connecting hub between these two signaling pathways. Further supporting these findings was the observation that ERK1/2 inhibition diminished all forms of p90RSK expression, followed by decreased mTOR signaling (Supplementary Fig. S4B).

Inhibition of p90RSK in ganetespib-resistant cells, genetically or pharmacologically, induces synthetic lethality, whereas overexpression in naïve parental cells results in resistance

Our results strongly suggest that p90RSK activity and expression were critical for mediating the observed resistance. To validate our findings, we first expressed shRNAs to silence individual

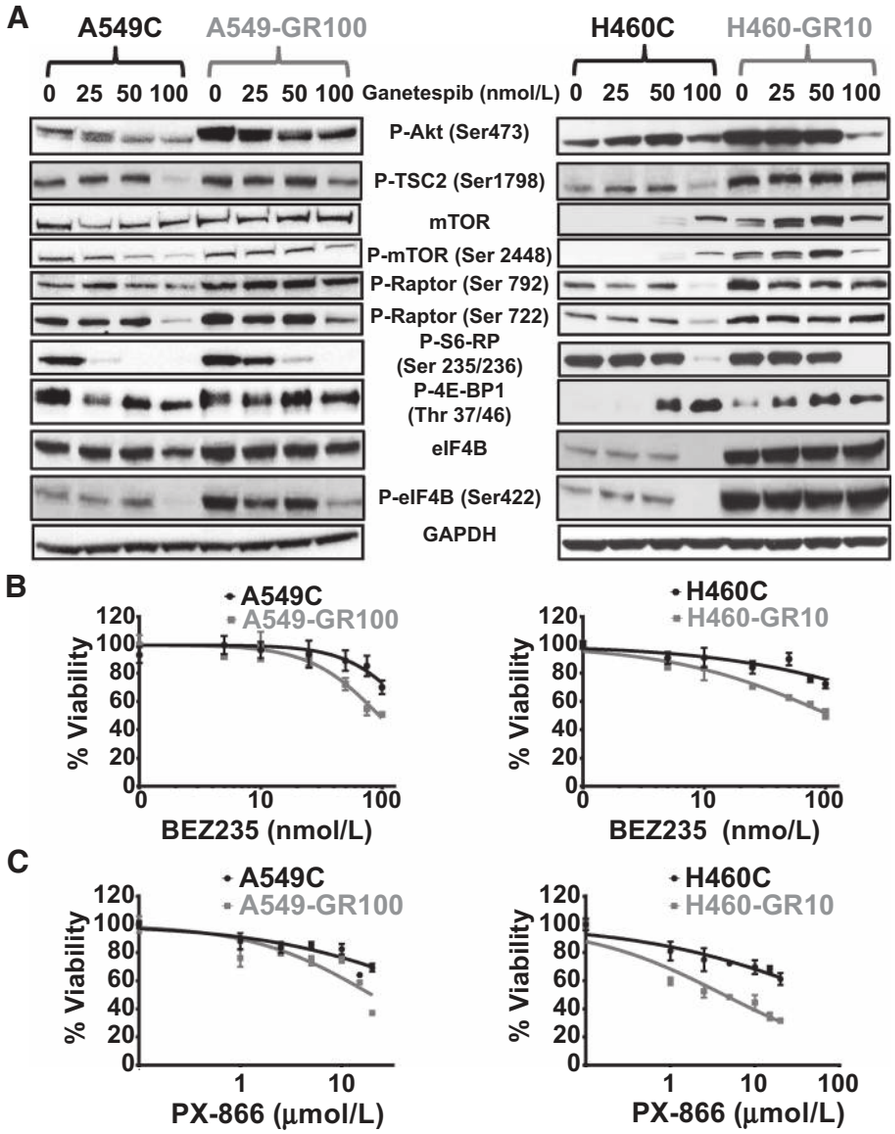

Figure 4.
Ganetespib resistance induces hyperactivation of the AKT/mTOR pathway, leading to PI3K/mTOR dependence. **A,** Expression of mTOR pathway proteins were assessed by immunoblotting in control (C) versus ganetespib-resistant cells, after they were exposed to increasing concentrations of ganetespib for 48 hours. GAPDH was included as loading control. Percent viabilities of ganetespib-resistant cells in comparison with control cells in response to increasing concentrations of PI3K/mTOR dual inhibitor BEZ235 (0–100 nmol/L; **B**) and PI3K inhibitor PX-866 (0–20 μmol/L; **C**) were determined by MTS assay after the cells were treated with the drug for 72 hours.

p90RSK isoforms (Supplementary Fig. S5A) to determine the relative contribution of each isoform, as we observed increased activity of all isoforms in our ganetespib-resistant cells. We observed that although the ganetespib-resistant cells can tolerate the loss of a single isoform in the absence of ganetespib, targeting even one RSK isoform is sufficient to sensitize them to ganetespib (Fig. 6A) compared with control cells. Next, to further corroborate our finding, ganetespib-resistant cells were treated with two well-characterized and specific inhibitors of p90RSK, BI-D1870 (25) and SL0101 (26). Interestingly, although these inhibitors had little activity as monotherapy in the parental cells, they demonstrated significant cytotoxicity in A549-GR100 and H460-GR10 (Fig. 6B; Supplementary Table S3). To further support that the observed cytotoxicity of BI-D1870 was not due off-target effects of this agent, we examined the effect of BI-D1870 on RSK activity at the doses at which we observed growth inhibition. We observed dose-dependent decrease in the activities of all four isoforms in control and ganetespib-resistant cells, which directly correlated with the observed cytotoxicity (Supplementary Fig. S6). To validate p90RSK's involvement in resistance mechanism, we overexpressed individual p90RSK isoforms in parental A549 cells (Supplementary Fig. S5B) and examined whether they could induce ganetespib resistance. Interestingly, overexpression of a subset of isoforms (1, 2, 4) led to significant ganetespib resistance (Fig. 6C), suggesting that p90RSK is one of the key factors mediating the acquired resistance to ganetespib.

To establish the role of p90RSK in ganetespib resistance *in vivo* and to examine whether overexpression of one of the isoform would be sufficient enough to induce the resistance, we implanted A549-W118Δ (control) and A549-RSK1A–overexpressing cells in mice to form tumors, which we subsequently treated with ganetespib or vehicle (DMSO; Fig. 6D). A linear mixed effects model with random intercept predicted tumor volume (log, base 2) by cell line (A549-W118Δ vs. A549-RSK1A), treatment (vehicle vs. ganetespib), and time (continuous, days 1, 4, 7, 10, 14, 18, and 21) was used. With only vehicle treatment, there was not a

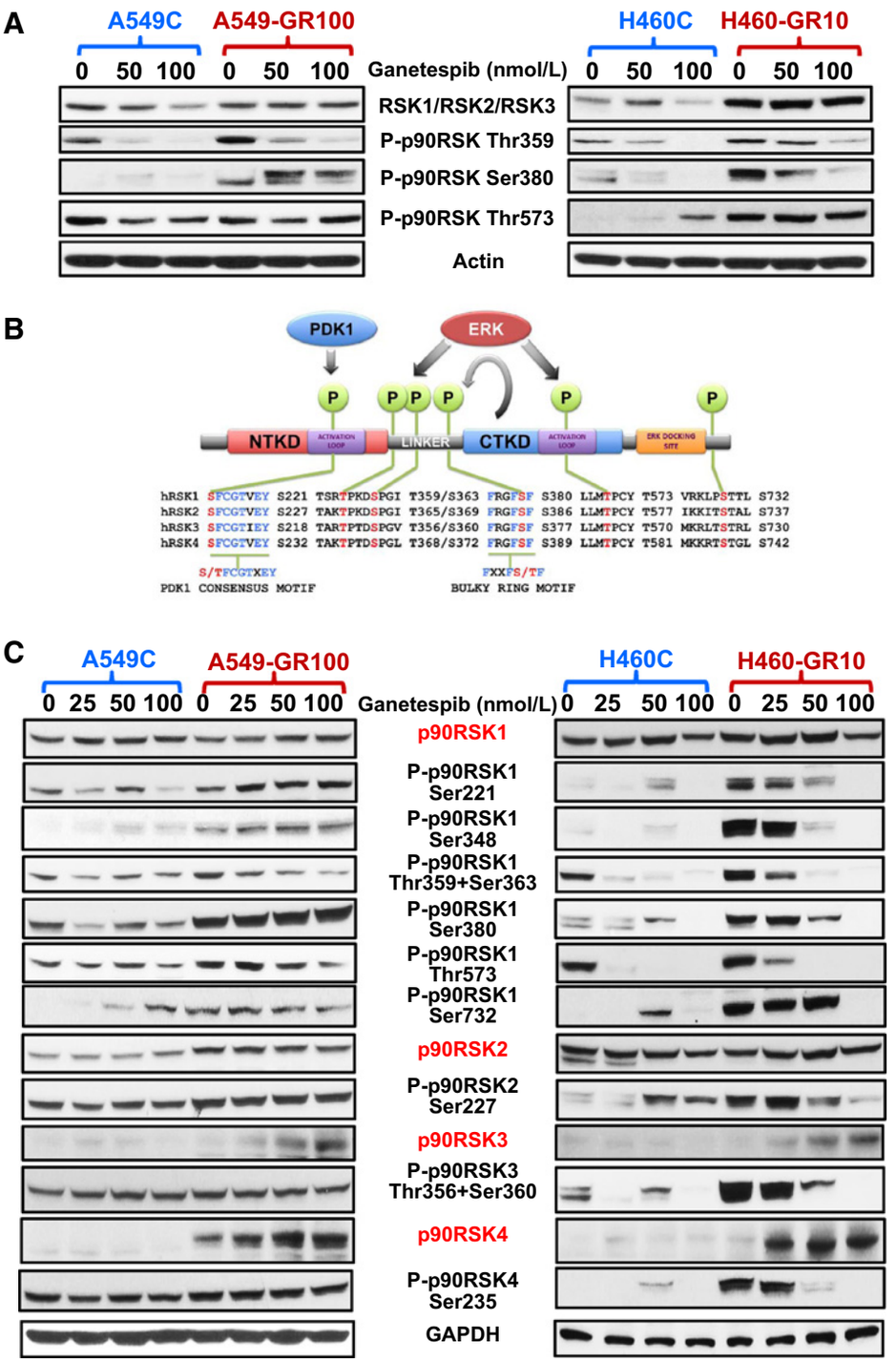

Figure 5.
Acquired resistance to ganetespib results in increased activity and expression of p90RSK and its isoforms in *KRAS*-mutant ganetespib-resistant NSCLC cells. **A,** p90RSK activity after ganetespib treatment (48 hours) in control (C) and ganetespib-resistant cells was analyzed by immunoblotting using total and phospho-specific pan-p90RSK antibodies as indicated. Actin was included as loading control. **B,** Comparative illustration of p90RSK isoform structure indicating key phosphorylation sites required for its activation. **C,** Expression of p90RSK isoforms after ganetespib treatment (48 hours) in control and ganetespib-resistant cells was assessed by immunoblotting using total isoform–specific (red) and phosphorylation isoform–specific (black) antibodies as stated, and GAPDH was used as loading control.

significant difference in growth rates between cell lines as the predicted average doubling time for both cell lines was 9 days (95% CI, 8–10). However, with ganetespib treatment, there was a significant difference in growth between the A549-W118Δ and A549-RSK1A cell lines as the average doubling time for A549-RSK1A tumors was 10 days (95% CI, 9–11; Wald $P = 0.11$ for treatment effect within cell line) and for A549-W118Δ was 17 days (95% CI, 14–20; $P < 0.001$). These results strongly suggest that overexpression of even one isoform of the protein can induce significant ganetespib resistance both *in vitro* and *in vivo*.

Discussion

Clinical advances in the treatment of lung cancer have come from the recognition that NSCLC is a collection of distinct molecularly driven neoplasms, not a single disease entity. Such

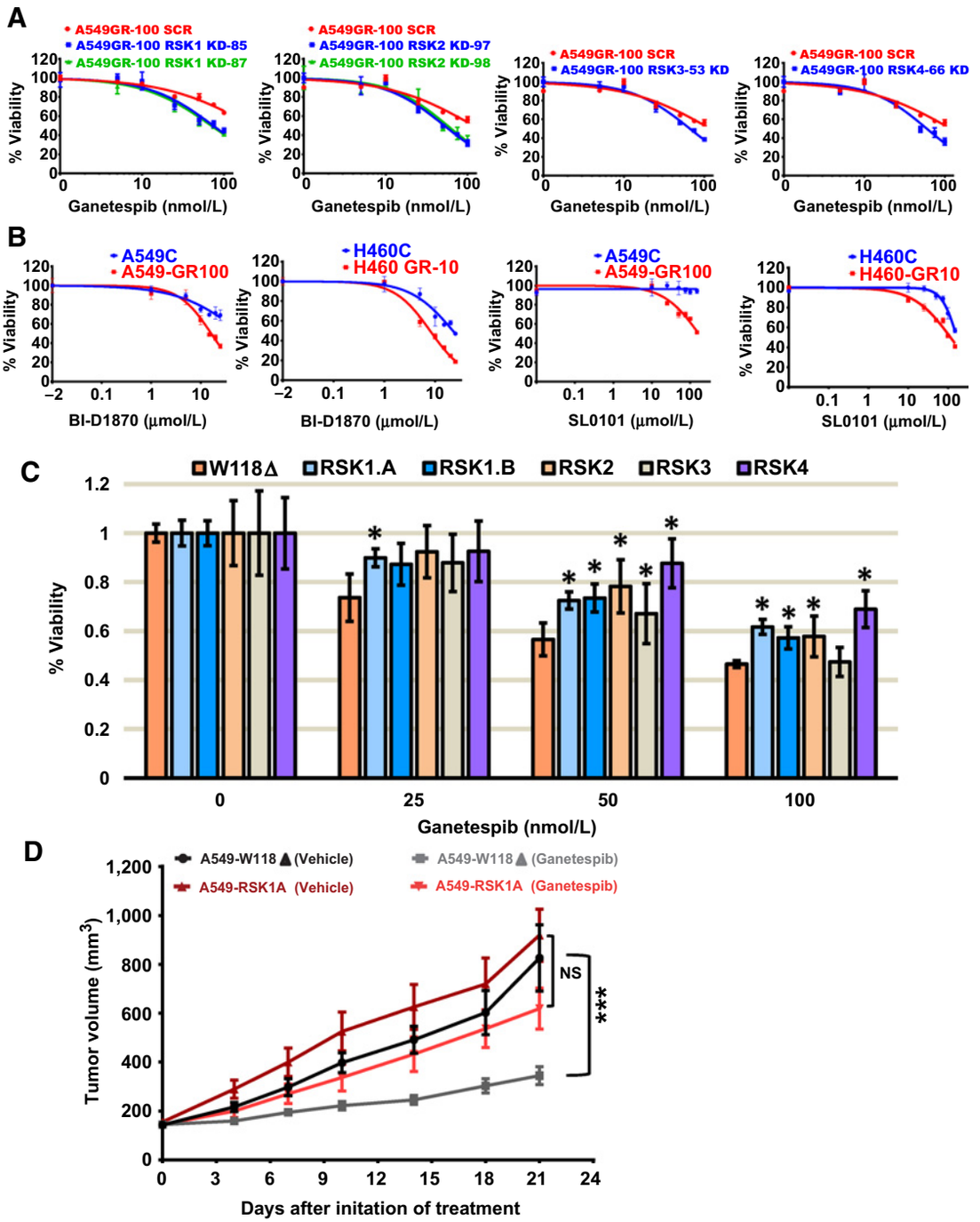

Figure 6.

Ganetespib-resistant cells are dependent upon p90RSK signaling, and overexpression of an individual p90RSK isoform is sufficient to induce ganetespib resistance. **A,** Individual p90RSK isoforms were silenced in A549-GR100 cells by expressing specific shRNA, and percent viability was measured by MTS assays after 72 hours of treatment with increasing concentrations of ganetespib. A549-GR100 cells expressing scramble shRNA (SCR) were used as a negative control. **B,** Percent viability of A549 and H460 ganetespib-resistant cells in comparison with control parental cells after 72 hours of treatment with the pan-RSK inhibitors, BI-D1870 (0–25 μmol/L; left) and SL0101 (0–150 μmol/L; right) was determined by MTS assay. **C,** p90RSK isoform–specific ORFs were individually expressed in A549C parental cells, and percent viability were assessed by MTS assays after 48 hours of treatment with specific ganetespib doses (0, 25, 50, and 100 nmol/L). A549C cells expressing empty vector, W118Δ, were used as a negative control. Bars, mean percent cell viability (± SD) relative to the mean of control cells. Each cell type in each experiment included four replicates. Statistical significance by paired Student *t* test is denoted as *, $P < 0.05$. **D,** Ganetespib-induced tumor regression was compared between control A549 xenografts arms either overexpressing empty vector W118Δ or the ORF of p90RSK-1A isoform. Tumor growth curves represent mean tumor volume (±SEM). Seven mice per treatment arm, except for W118Δ receiving ganetespib (8). Linear contrasts in a random intercept linear mixed model indicate a greater treatment group difference in the W118Δ model (86% greater doubling time with ganetespib treatment) than for RSK1A (12% greater doubling time; Wald ***, $P < 0.001$). NS, not significant.

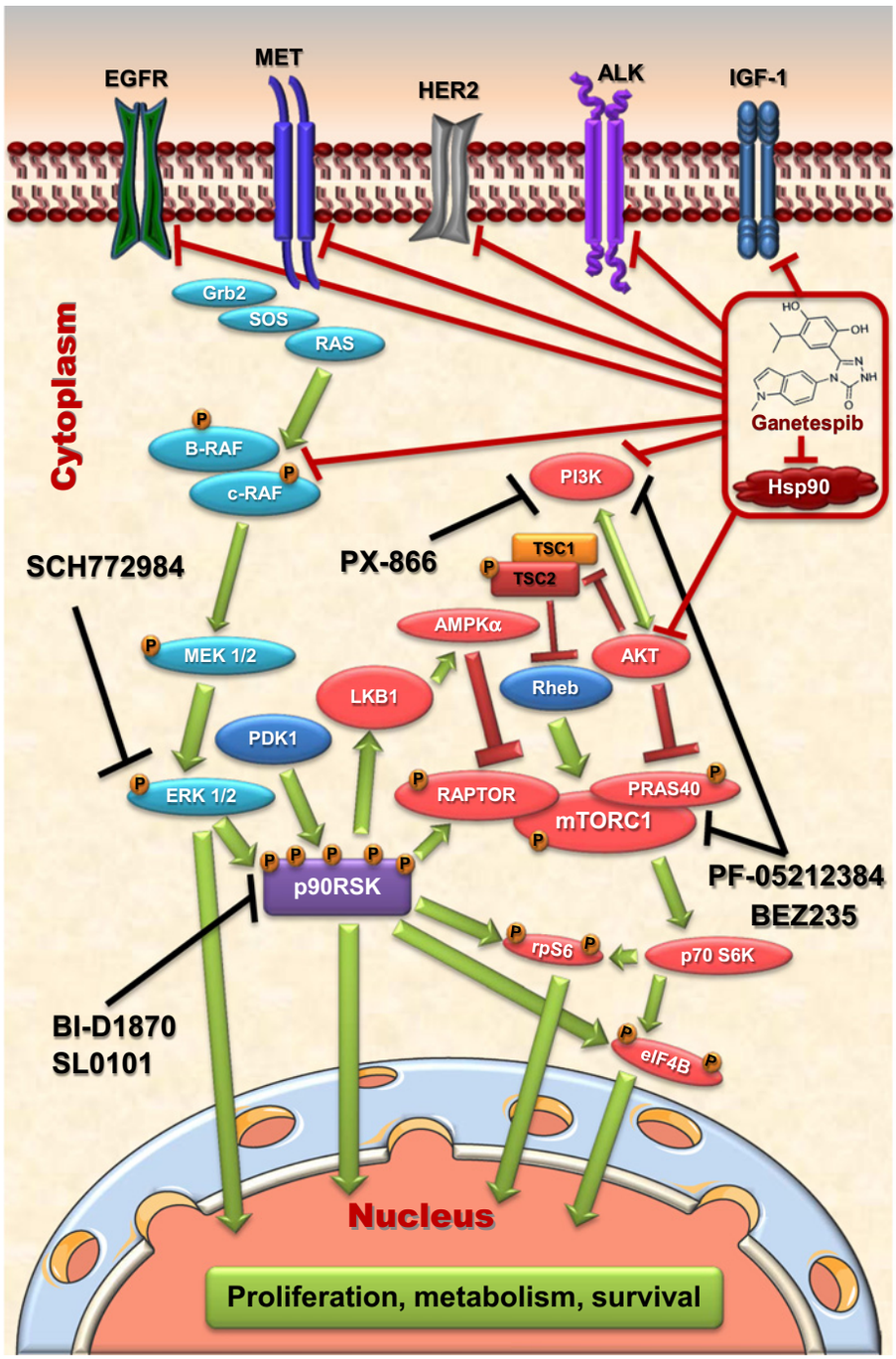

Figure 7.
Potential therapeutic combinations involving Hsp90 inhibitor ganetespib to overcome acquired ganetespib resistance. In *KRAS*-mutant NSCLC, acquired resistance to ganetespib is mediated via hyperactivation of ERK and mTOR pathways. Targeted inhibition of PI3K/mTOR or ERK1/2 or p90RSK induced synthetic lethality in ganetespib-resistant cells. On the basis of our results, this model illustration proposes that combination of HSP90i, ganetespib with inhibitors of PI3K (PX866), PI3K/mTOR (BEZ235) or p90RSK (SL0101 or BI-D1870), or an inhibitor for ERK1/2 (SCH772984) may prevent ganetespib resistance and/or help overcome the resistance after single-agent treatment. Although not shown in this figure, MEK, PDK1, and p90RSK are also direct targets of Hsp90 inhibition.

approaches based on the molecular background of the tumor in NSCLC patients have led to the approval by the FDA of EGFR TKIs in *EGFR*-mutant lung adenocarcinomas and ALK inhibitors in *ALK*-rearranged lung adenocarcinomas (27). Unfortunately, there is no effective therapy for the most common oncogenic driver in NSCLC mutant *KRAS*. Thus, there is a critical need for novel agents targeting *KRAS*-mutant NSCLC. In this report, we focused on determining the molecular mechanisms responsible for acquired ganetespib resistance in *KRAS*-mutant NSCLC and propose a rational approach to overcome such resistance. These studies are essential for Hsp90 inhibitors to go forward in clinical development, as Hsp90 inhibitor combinations tested in the clinic to date have been empirically paired with standard-of-care chemotherapy. Previous combinations not based upon an understanding of mechanisms of Hsp90 resistance have resulted in disappointing and discouraging negative phase III trials, including a recent large phase III trial looking at the combination of ganetespib with docetaxel in advanced adenocarcinoma of the lung (5).

Therefore, we explored the molecular mechanisms underlying ganetespib resistance studying three ganetespib resistant *KRAS*-mutant NSCLC cell lines. We have established the hyperactivation of RAF/MEK/ERK and PI3K/AKT/mTOR signaling as the foundation of the resistance mechanism. These findings provided us with a number of molecular targets we could select to combine with ganetespib monotherapy to overcome the resistance (Fig. 7). mTOR serves as a master switch of cell growth and metabolism and many other signaling pathways including RAS/RAF/ERK lead to mTOR activation. Ganetespib-resistant cells also exhibited increased dependence on these pathways, as these cells showed synthetic lethality to the targeted pharmacologic inhibitions by PF-05212384, BEZ235, PX-866, and SCH772984. Interestingly, several previous reports have suggested that the combination of an Hsp90i and mTOR or dual PI3K/mTOR inhibitor may be efficacious *in vitro* and *in vivo* (12, 28).

In addition, we observed significant activity with the ERK inhibitor SCH772984. Currently, at least two ERK1/2 inhibitors are in phase I trials, MK8353 (NCT01358331) and BVD523 (NCT01781429). Our preclinical studies on SCH772984 suggest that the combination of an Hsp90 inhibitor with an ERK inhibitor would be a rational combination to explore in the clinic. Alternatively, several MEK inhibitors are FDA approved for melanoma and are being tested currently in NSCLC. Interestingly, the MEK inhibitor selumetinib has demonstrated significant activity in combination with docetaxel in *KRAS*-mutant NSCLC (29). In addition, the dual inhibitor of PI3K/mTOR, PF-05212384, is currently being investigated in several phase I and II studies (NCT00940498, NCT02920450, NCT01920061), where it is being tested in combination with a variety of cytotoxic and targeted agents.

The most striking part of our finding is the involvement of the p90RSK family of proteins in mediating the acquired resistance to ganetespib in *KRAS*-mutant NSCLC. Upon activation by ERK1/2 and PDK1, p90RSK proteins proceed to activate a vast array of substrates. Although there is evidence suggesting that RAF/MEK/ERK pathway activation may inhibit AKT signaling (30), cross-activation of PI3K/AKT/mTOR either directly by ERK activation or via p90RSK activation leading to activation of mTORC1 has also been well documented (31, 32). Our results demonstrating increased activity and expression in some cases for all four p90RSK isoforms in our ganetespib-resistant cell lines (Fig. 5) suggest that p90RSK is an important mediator of resistance. This is further supported by the ability of isoform-specific p90RSK knockdown in ganetespib-resistant cells to resensitize to ganetespib, and conversely, overexpression of individual RSK isoforms led to *de novo* ganetespib resistance i*n vitro* and *in vivo*. Furthermore, targeted pharmacologic inhibition of p90RSK with BI-D1870 or SL0101 resulted in synthetic lethality in ganetespib-resistant cells (Fig. 6). In this article, we have not identified the key p90RSK substrate(s) that are responsible for inducing resistance to ganetespib; however, we are actively pursuing these targets. p90RSK family has been implicated in the regulation of cell growth and protein synthesis, cell migration and survival, cell proliferation, and cell-cycle progression and in some cases drug efflux (24, 33, 34). Although it is less likely that p90RSK is mediating resistance through increased drug efflux given our results in Supplementary Fig. S2, it could still be possible that p90RSK1-induced upregulation of P-glycoprotein may contribute to the observed resistance via drug efflux as recently described by Katayama and colleagues (34). These findings not only secure its role in mediating ganetespib resistance in *KRAS*-mutant NSCLC, but also identify p90RSK as a central targetable node to prevent or overcome resistance.

In conclusion, our preclinical work suggests that the combination of ganetespib with an ERK1/2 inhibitor, PI3K inhibitor, dual PI3K/mTOR inhibitor, or an RSK inhibitor would be an effective strategy to test in the clinic (Fig. 7). Information on the *in vivo* use of the p90RSK inhibitors is lacking; therefore, further preclinical development of these agents is necessary before they can be tested in the clinic. The combination of ganetespib or even other Hsp90i currently in clinical trials (e.g., AT13387) with any one of the inhibitors tested in this study may prevent ganetespib resistance and/or help overcome the resistance after single-agent treatment. These studies provide preclinical rationale for a future phase I/II trial in *KRAS*-mutant NSCLC testing these therapeutic combinations.

Disclosure of Potential Conflicts of Interest

No potential conflicts of interest were disclosed.

Authors' Contributions

Conception and design: S. Chatterjee, T.F. Burns
Development of methodology: S. Chatterjee, T.F. Burns
Acquisition of data (provided animals, acquired and managed patients, provided facilities, etc.): S. Chatterjee, E.H.-B. Huang, I. Christie, T.F. Burns
Analysis and interpretation of data (e.g., statistical analysis, biostatistics, computational analysis): S. Chatterjee, E.H.-B. Huang, I. Christie, B.F. Kurland, T.F. Burns
Writing, review, and/or revision of the manuscript: S. Chatterjee, B.F. Kurland, T.F. Burns
Administrative, technical, or material support (i.e., reporting or organizing data, constructing databases): S. Chatterjee, E.H.-B. Huang, I. Christie
Study supervision: T.F. Burns
Other (animal tumor PDX and xenograft experiment and drug evaluation): E.H.-B. Huang

Acknowledgments

The authors thank Mark Socinski, MD; James G. Herman, MD; Laura Stabile, PhD; Deborah L. Galson, PhD; Peter Wipf, PhD; Frank P. Vendetti, PhD; Juraj Adamik, PhD; Zachary A. Yochum, B.S., at the University of Pittsburgh and David Proia formerly of Synta Pharmaceuticals for the discussion, advice regarding this work, and supply of resources when applicable. They also thank Synta Pharmaceuticals Corp. for the constant supply of ganetespib.

Grant Support

T.F. Burns and S. Chatterjee have received research funding for this project from a LUNGevity Foundation Career Development Award and a UPCI LUNG SPORE CDA P50CA090440. This project used the UPCI Animal and Biostatistics Facilities that are supported in part by award P30CA047904.

The costs of publication of this article were defrayed in part by the payment of page charges. This article must therefore be hereby marked *advertisement* in accordance with 18 U.S.C. Section 1734 solely to indicate this fact.

Received October 13, 2016; revised January 23, 2017; accepted January 25, 2017; published OnlineFirst February 6, 2017.

References

1. Siegel RL, Miller KD, Jemal A. Cancer statistics, 2016. CA Cancer J Clin 2016;66:7–30.
2. Cox AD, Der CJ. Ras family signaling: therapeutic targeting. Cancer Biol Ther 2002;1:599–606.
3. Riely GJ, Marks J, Pao W. KRAS mutations in non-small cell lung cancer. Proc Am Thoracic Soc 2009;6:201–5.
4. Young A, Lyons J, Miller AL, Phan VT, Alarcon IR, McCormick F. Ras signaling and therapies. Adv Cancer Res 2009;102:1–17.

5. Chatterjee S, Bhattacharya S, Socinski MA, Burns TF. HSP90 inhibitors in lung cancer: promise still unfulfilled. Clin Adv Hematol Oncol 2016; 14:346–56.
6. Neckers L, Workman P. Hsp90 molecular chaperone inhibitors: are we there yet? Clin Cancer Res 2012;18:64–76.
7. Sequist LV, Gettinger S, Senzer NN, Martins RG, Janne PA, Lilenbaum R, et al. Activity of IPI-504, a novel heat-shock protein 90 inhibitor, in patients with molecularly defined non-small-cell lung cancer. J Clin Oncol 2010;28:4953–60.
8. Socinski MA, Goldman J, El-Hariry I, Koczywas M, Vukovic V, Horn L, et al. A multicenter phase II study of ganetespib monotherapy in patients with genotypically defined advanced non-small cell lung cancer. Clin Cancer Res 2013;19:3068–77.
9. Burns TF, Dobromilskaya I, Murphy SC, Gajula RP, Thiyagarajan S, Chatley SN, et al. Inhibition of TWIST1 leads to activation of oncogene-induced senescence in oncogene-driven non-small cell lung cancer. Mol Cancer Res 2013;11:329–38.
10. Moffat J, Grueneberg DA, Yang X, Kim SY, Kloepfer AM, Hinkle G, et al. A lentiviral RNAi library for human and mouse genes applied to an arrayed viral high-content screen. Cell 2006;124:1283–98.
11. Sarbassov DD, Guertin DA, Ali SM, Sabatini DM. Phosphorylation and regulation of Akt/PKB by the rictor-mTOR complex. Science 2005;307: 1098–101.
12. Acquaviva J, Smith DL, Sang J, Friedland JC, He S, Sequeira M, et al. Targeting KRAS-mutant non-small cell lung cancer with the Hsp90 inhibitor ganetespib. Mol Cancer Ther 2012;11:2633–43.
13. Acquaviva J, He S, Zhang C, Jimenez JP, Nagai M, Sang J, et al. FGFR3 translocations in bladder cancer: differential sensitivity to HSP90 inhibition based on drug metabolism. Mol Cancer Res 2014;12:1042–54.
14. Banz VM, Medova M, Keogh A, Furer C, Zimmer Y, Candinas D, et al. Hsp90 transcriptionally and post-translationally regulates the expression of NDRG1 and maintains the stability of its modifying kinase GSK3beta. Biochim Biophys Acta 2009;1793:1597–603.
15. Jin J, Tian R, Pasculescu A, Dai AY, Williton K, Taylor L, et al. Mutational analysis of glycogen synthase kinase 3beta protein kinase together with kinome-wide binding and stability studies suggests context-dependent recognition of kinases by the chaperone heat shock protein 90. Mol Cell Biol 2016;36:1007–18.
16. Morris EJ, Jha S, Restaino CR, Dayananth P, Zhu H, Cooper A, et al. Discovery of a novel ERK inhibitor with activity in models of acquired resistance to BRAF and MEK inhibitors. Cancer Discov 2013;3:742–50.
17. Wong DJ, Robert L, Atefi MS, Lassen A, Avarappatt G, Cerniglia M, et al. Antitumor activity of the ERK inhibitor SCH772984 [corrected] against BRAF mutant, NRAS mutant and wild-type melanoma. Mol Cancer 2014;13:194.
18. Inoki K, Li Y, Zhu T, Wu J, Guan KL. TSC2 is phosphorylated and inhibited by Akt and suppresses mTOR signalling. Nat Cell Biol 2002;4:648–57.
19. Potter CJ, Pedraza LG, Xu T. Akt regulates growth by directly phosphorylating Tsc2. Nat Cell Biol 2002;4:658–65.
20. Ma L, Chen Z, Erdjument-Bromage H, Tempst P, Pandolfi PP. Phosphorylation and functional inactivation of TSC2 by Erk implications for tuberous sclerosis and cancer pathogenesis. Cell 2005;121:179–93.
21. Cargnello M, Roux PP. Activation and function of the MAPKs and their substrates, the MAPK-activated protein kinases. Microbiol Mol Biol Rev 2011;75:50–83.
22. Roux PP, Blenis J. ERK and p38 MAPK-activated protein kinases: a family of protein kinases with diverse biological functions. Microbiol Mol Biol Rev 2004;68:320–44.
23. Carriere A, Cargnello M, Julien LA, Gao H, Bonneil E, Thibault P, et al. Oncogenic MAPK signaling stimulates mTORC1 activity by promoting RSK-mediated raptor phosphorylation. Curr Biol 2008;18:1269–77.
24. Romeo Y, Zhang X, Roux PP. Regulation and function of the RSK family of protein kinases. Biochem J 2012;441:553–69.
25. Sapkota GP, Cummings L, Newell FS, Armstrong C, Bain J, Frodin M, et al. BI-D1870 is a specific inhibitor of the p90 RSK (ribosomal S6 kinase) isoforms in vitro and in vivo. Biochem J 2007;401:29–38.
26. Smith JA, Poteet-Smith CE, Xu Y, Errington TM, Hecht SM, Lannigan DA. Identification of the first specific inhibitor of p90 ribosomal S6 kinase (RSK) reveals an unexpected role for RSK in cancer cell proliferation. Cancer Res 2005;65:1027–34.
27. Somasundaram A, Socinski MA, Burns TF. Personalized treatment of EGFR mutant and ALK-positive patients in NSCLC. Expert Opin Pharmacother 2014;15:2693–708.
28. De Raedt T, Walton Z, Yecies JL, Li D, Chen Y, Malone CF, et al. Exploiting cancer cell vulnerabilities to develop a combination therapy for ras-driven tumors. Cancer Cell 2011;20:400–13.
29. Jänne PA, Shaw AT, Pereira JR, Jeannin G, Vansteenkiste J, Barrios C, et al. Selumetinib plus docetaxel for KRAS-mutant advanced non-small-cell lung cancer: a randomised, multicentre, placebo-controlled, phase 2 study. Lancet Oncol 2013;14:38–47.
30. Jiang Z, Zhang Y, Chen X, Lam PY, Yang H, Xu Q, et al. Activation of Erk1/2 and Akt in astrocytes under ischemia. Biochem Biophys Res Commun 2002;294:726–33.
31. Carriere A, Romeo Y, Acosta-Jaquez HA, Moreau J, Bonneil E, Thibault P, et al. ERK1/2 phosphorylate Raptor to promote Ras-dependent activation of mTOR complex 1 (mTORC1). J Biol Chem 2011;286:567–77.
32. Zoncu R, Efeyan A, Sabatini DM. mTOR: from growth signal integration to cancer, diabetes and ageing. Nat Rev Mol Cell Biol 2011;12:21–35.
33. Anjum R, Blenis J. The RSK family of kinases: emerging roles in cellular signalling. Nat Rev Mol Cell Biol 2008;9:747–58.
34. Katayama K, Fujiwara C, Noguchi K, Sugimoto Y. RSK1 protects P-glycoprotein/ABCB1 against ubiquitin-proteasomal degradation by downregulating the ubiquitin-conjugating enzyme E2 R1. Sci Rep 2016;6:36134.